The Electrostatic Potential Profile in a Tandem Mirror Thermal Barrier

X.Z. Li and G.A. Emmert

November 1980

UWFDM-392

FUSION TECHNOLOGY INSTITUTE

UNIVERSITY OF WISCONSIN

MADISON WISCONSIN

The Electrostatic Potential Profile in a Tandem Mirror Thermal Barrier

X.Z. Li and G.A. Emmert

Fusion Technology Institute
University of Wisconsin
1500 Engineering Drive
Madison, WI 53706

http://fti.neep.wisc.edu

November 1980

UWFDM-392

The Electrostatic Potential Profile in a Tandem Mirror Thermal Barrier

by
X.Z. Li*
and
G.A. Emmert
Fusion Engineering Program
Department of Nuclear Engineering
University of Wisconsin
Madison, Wisconsin

November 1980

UWFDM- 392

*Visiting Scholar from Southwestern Institute of Physics, Leshan, Sichuan, China.

Presented at 22nd annual meeting of the Division of Plasma Physics, American Physical Society, 10-14 November 1980, San Diego, CA.

Abstract

The electrostatic potential profile in the thermal barrier is calculated using a collisional model for the ion distribution function. It is seen that this model gives a continuous potential profile near the barrier magnetic field peak, unlike other works which have yielded a discontinuous potential there. Between the barrier magnetic field minimum and the plug, the electron distribution function is taken to be piecewise Maxwellian at the central cell and plug electron temperatures. Using this model, the electrostatic potential profile from the barrier peak field to the plug mirror throat is calculated.

I. Introduction

The thermal barrier[1] is a region of reduced magnetic field strength and density between the end-plug and central cell of a tandem mirror. The thermal barrier allows the electrons in the plug to be heated to a higher temperature than those in the central cell and consequently permits one to obtain an electrostatic potential peak in the plugs even when the plug density is less than the central cell density. This greatly improves the Q (ratio of fusion power to total injected power) and reduces the need for high magnetic fields in the end-plugs. These improvements are a significant advance in the tandem mirror confinement scheme.

Successful operation of the thermal barrier requires that the density of trapped ions in the barrier be kept small by some pumping mechanism which either removes them from the plasma, as in drift-orbit pumping,[2] or converts them back to passing ions, as in neutral beam[3] or RF pumping.[4]

The thermal barrier concept presents a variety of physics questions requiring further analysis. Among these are the electrostatic potential profile in the barrier. The electrostatic potential plays an important role in determining the parallel motion of the trapped ions in the barrier, and hence has an effect on their drift motion. Knowledge of the latter is required for assessing the efficiency of drift orbit pumping. The electrostatic potential profile along magnetic field lines also determines the turning point of the passing ions and hence determines the effective volume of the barrier. This is needed in 0-D codes which calculate the performance of tandem mirrors.

The electrostatic profile in the thermal barrier has been analyzed by Kesner[5] using the assumption of a piece-wise Maxwellian distribution for the passing ions, with the trapped ions treated phenomenologically through a

parameter γ. The limit $\gamma \to 0$ is the limit of no trapped ions in the barrier, i.e., perfect pumpout. Kesner then calculates the potential as a function of the mirror ratio (B_{mb}/B) and γ. Here B is the local magnetic field strength and B_{mb} is its value at the peak field in the barrier. Kesner found the surprising (and unphysical) result that as $B \to B_{mb}$, the potential $\phi \to -.77\ T_e$ whereas it was taken to be zero at B_{mb}. Hence the potential drops discontinuously at the beginning of the barrier in his calculation. Cohen[6] used a model trapped ion distribution function which was chosen to resemble the results of Fokker-Planck calculations[7] and to connect to a Maxwellian distribution function for the passing ions. His calculations show no discontinuity in the potential near the barrier peak field, except in the limit of very small trapped ion density (smaller than expected attainable values).

Both of the above papers treat only the part of the barrier on the central cell side of the minimum field point. In this paper we consider the potential profile not only on the central cell side, but also on the plug side of the minimum field point. In this region there are 2 classes of electrons: the first are the passing electrons from the central cell and the second are the plug electrons whose turning points lie in the barrier. These two classes cause the electron distribution function to be piece-wise Maxwellian, but with different "temperatures" in different regions of velocity space. These regions must be connected by a collisional boundary layer at the interface between them. We also use a different model for the distribution function of the trapped and passing ions. The result of our calculation is a continuous and smooth axial potential profile from the barrier magnetic field peak through the minimum field point to the mirror throat of the plug, where the density of hot, magnetically confined ions begins to rise.

II. The Model

A schematic of the axial magnetic field and potential profile for an inboard thermal barrier is shown in Figure 1. We consider only the inboard configurations in this report, although similar concepts apply also to other barrier configurations.

The basic assumption made is that the bounce frequency for trapped (or passing) particles in the thermal barrier is much greater than the collision frequency. Consequently, particle dynamics is assumed to be collisionless. The parallel motion is described using guiding center theory with the magnetic moment, μ, treated as a constant of the motion (i.e., an adiabatic invariant) along with the total particle energy, E. The ion distribution function is assumed to have relaxed to a collisional distribution function since the equilibrium lasts for times longer compared with the mean collision time. Shown in Fig. 2 is the E-μ space for ions in the thermal barrier. Ions in Region I are passing ions; they have sufficient energy and low enough μ to penetrate the barrier peak field and enter the central cell. Ions in Regions II and III are trapped in the barrier. Ions in Region IV would also be trapped, but it is assumed that this region is unpopulated because of barrier pumping. Pumping is treated phenomenologically by imposing the boundary condition that the ion distribution function vanish along the line A in Fig. 2. Region III differs from Region II in that ions can scatter from Region I to Region II by pitch angle scattering, but can only get to Region III by scattering in energy.

We define a series of μ's as:

$$\mu_{mb} = \frac{E - e\phi_{mb}}{B_{mb}}$$

$$\mu_o = \frac{E-e\phi_o}{B_o}$$

$$\mu_1 = \mu + \frac{e\phi_{mb}-E}{B_o} \quad , \tag{1}$$

and a series of pitch angles as

$$\theta^c = \sin^{-1} \left(\frac{\mu B_c}{E-e\phi_c}\right)^{1/2}$$

$$\theta^c_{mb} = \sin^{-1} \left(\frac{\mu_{mb} B_c}{E-e\phi_c}\right)^{1/2}$$

$$\theta^b = \sin^{-1} \left(\frac{\mu B_b}{E-e\phi_b}\right)^{1/2}$$

$$\theta^b_{mb} = \sin^{-1} \left(\frac{\mu_{mb} B_b}{E-e\phi_b}\right)^{1/2}$$

$$\theta^b_o = \sin^{-1} \left(\frac{\mu_o B_b}{E-e\phi_b}\right)^{1/2}$$

$$\theta^b_1 = \sin^{-1} \left(\frac{\mu_1 B_b}{e\phi_{mb}-e\phi_b}\right)^{1/2}$$

$$\theta^b_{10} = \sin^{-1} \left(\frac{e\phi_{mb}-e\phi_o}{B_o} \quad \frac{B_b}{(e\phi_{mb}-e\phi_b)}\right)^{1/2} . \tag{2}$$

The angles θ^c and θ^b are the pitch angles measured at the midplane of the central cell and the bottom of the barrier, respectively. The angles θ^c_{mb} and θ^b_{mb} are the loss-cone angles corresponding to the mirror ratio betweeen the barrier peak and the central cell, or bottom of the barrier, respectively.

The ion distribution function in the barrier is obtained by using a pitch

angle scattering operator in the Fokker-Planck equation. The effect of barrier pumping is treated in a rather phenomenological manner by introducing the boundary condition that the distribution function vanishes at the pitch angle $\theta^b = \theta^b_o$. The result is

$$F_i(E,\theta^b) = \begin{cases} \{c_2 \log\left[\dfrac{\cos(\frac{\theta^c}{2})}{\cos(\frac{\theta^c_{mb}}{2})}\right] + c_t \log\left[\dfrac{\tan(\frac{\theta^b_o}{2})}{\tan(\frac{\theta^b_{mb}}{2})}\right]\} e^{-E/T_{ic}} & \text{(Region I)} \\ c_t \log\left[\dfrac{\tan(\frac{\theta^b_o}{2})}{\tan(\frac{\theta^b}{2})}\right] e^{-E/T_{ic}} & \text{(Region II)} \\ c_t \log\left[\dfrac{\tan(\frac{\theta^b_{10}}{2})}{\tan(\frac{\theta^b_1}{2})}\right] e^{-|E-e\phi_{mb}|/T_{ic}} . & \text{(Region III)} \end{cases} \quad (3)$$

The part in Region III, which cannot be reached by simple pitch angle scattering, is chosen to match continuously at the interface between Regions II and III the value of F_i in Region II. It is also chosen to agree qualitatively with Fokker-Planck calculations of the barrier.[7]

Since the thermal barrier appears as a potential "hill" to the electrons, they are treated differently than the ions. Between the barrier minimum and the central cell, the electrons have a Maxwellian distribution and therefore satisfy the Boltzmann relationship between the electron density and potential using the central cell electron temperature, T_{ec}. We do not consider in this report the possibility of hot, magnetically trapped electrons in the barrier.

Between the barrier minimum and the plug, there are at least two classes

of electrons. First, there are electrons from the plug which are assumed to have come from a Maxwellian distribution at the plug electron temperature, T_{ep}. Second, there are electrons from the central cell which were sufficiently energetic to penetrate the barrier. These electrons are assumed to reflect off the falling potential on the other side of the plug and pass back through the barrier into the central cell. The E-μ phase space of the electrons between the barrier and the plug is shown in Fig. 3. The passing electrons from the central cell occupy Regions I and II and are assumed to have a Maxwellian distribution in I and II. The plug electrons occupy Region III in Fig. 3. Region IV corresponds to electrons which are electrostatically trapped by the barrier on one side and magnetically trapped by the plug on the other side. Since these electrons equilibrate more rapidly with the central cell electrons, we assign them the temperature T_{ec}. The electron distribution function is then taken as

$$f(E) = \begin{cases} F_c\, e^{-E/T_{ec}} & \text{(Regions I, II, IV)} \\ F_p\, e^{-E/T_{ep}} \,. & \text{(Region III)} \end{cases} \quad (4)$$

The coefficients F_c and F_p are determined by requiring that the electron density n_e, where

$$n_e(\phi,B) = \int d^3v\, f(E) \,, \quad (5)$$

reduces to the electron density at the barrier minimum and to the plug density

as one enters the plug. The electron density at the barrier minimum is given by the solution for the potential between the barrier minimum and the central cell. The plug density, plug potential, and central cell density are inputs to this calculation.

This completes the basic model used to calculate the potential profile in the thermal barrier. It differs from the work of Kesner[5] and Cohen[6] in two respects. First, we consider the potential profile on both sides of the barrier minimum. Second, the passing ion distribution is a collisional distribution, which approaches a Maxwellian distribution in the limit of poor barrier pumping, but deviates from a Maxwellian in the limit of good pumping. In particular, $F_i \to 0$ on the loss-cone boundary of passing ions when there are no trapped particles in the barrier. The models used by Cohen and Kesner were discontinuous in this limit.

III. Numerical Results

The electrostatic potential profile is obtained by invoking quasi-neutrality, i.e., $n_i(\phi,B) = n_e(\phi,B)$ and solving the resulting equation for $\phi(B)$, given the input parameters and the magnetic field profile.

First we consider the region between the barrier peak and the barrier minimum. In this region the electrons are Maxwellian and thus n_e depends only on ϕ and not B, while n_i depends on both. Fig. 4 shows the electron density and the ion density as a function of ϕ/T_{ec} (assuming $T_{ic}=T_{ec}=T_c$) for different magnetic field values (here $\tilde{B} = B/B_b$, where $B_{mb} = 10\ B_b$). The intersections give the value of ϕ for each B. For each value of B, there is only one solution and it approaches zero (the assumed potential at B_{mb}) as $B \to B_{mb}$. Consequently, we do not see the discontinuity in the potential found by Kesner[5] and Cohen.[6] These results are for the case of no trapped ions in the barrier.

If we had assumed that the passing ions had a Maxwellian distribution, then we would have gotten the curves shown in Fig. 5 (again for the case of no trapped ions). In this case $\phi \to -.77\ T_{ec}$ as $B \to B_{mb}$ and a second solution appears at $\phi=0$ for $B=B_{mb}$. This is the mathematical origin of the discontinuous solution found by Kesner.[5]

For the region between the barrier minimum and the plug, we use the piecewise Maxwellian distribution given in Eq. (4) for the electrons and get the result shown in Fig. 6. As B changes, there is only a single intersection which changes continuously, giving a continuous potential profile. An interesting mathematical peculiarity occurs if it is assumed that the electrons in Region IV of Fig. 3 are collisional equilibrium with the plug electrons rather than the central cell electrons and that the passing ions are Maxwellian. In this case one obtains the $n_i(\phi)$ and $n_e(\phi)$ curves of B, and one gets three solutions for ϕ (Fig. 7). This multiple-valuedness is nonphysical but perplexing. It does not occur if the Region IV electrons have temperature T_{ec}. A speculation concerning this difference in behavior is that the rate at which the electron distribution function makes the transition between satisfying a Boltzmann relation at temperature T_{ec} (e.g., near the bottom of the barrier) to a Boltzmann relation at temperature T_{ep} (e.g., in the plug) is significant. The rate of this transition is slower when Region IV electrons have temperature T_{ec}.

Fig. 8 shows the electrostatic potential profile from the barrier peak field to the plug mirror throat.

Acknowledgements

The authors gratefully acknowledge helpful discussions with Prof. J.D. Callen, Dr. J. Kesner, and Dr. J. Santarius. This research was supported in part by DOE.

References

1. D.E. Baldwin and B.G. Logan, Phys. Rev. Lett. 43 1318 (1979).
2. J. Kesner, Comments on Plasma Physics and Controlled Fusion 5 123 (1979).
3. D.E. Baldwin, B.G. Logan, T.C. Simonen, Editors, "Physics Basis for MFTF-B", Lawrence Livermore Laboratory Report UCID-18496 (1980).
4. Y. Matsuda, D.E. Baldwin, Bull. APS 24 1060 (1979).
5. J. Kesner, "Barrier Cell Sheath Formation," University of Wisconsin Report UWFDM-348 (1980).
6. R.H. Cohen, "Axial Potential Profiles in Thermal-Barrier Cells," LLNL Report UCRL-84535 (1980).
7. L. LoDestro, "Steady-State Ion Distributions in a Potential and Magnetic Well," Mirror Theory Monthly, Lawrence Livermore Laboratory (May 15, 1980).

Figure Captions

Fig. 1 The axial electrostatic potential and magnetic field profile in an inboard thermal barrier.

Fig. 2 E-μ phase space for ions.

Fig. 3 Electron phase space between the barrier minimum and the plug.

Fig. 4 Electron and ion density versus potential and magnetic field for the region between the barrier peak and the barrier minimum using the collisional ion distribution.

Fig. 5 Electron and ion density versus potential and magnetic field for the region between the barrier peak and the barrier minimum using a Maxwellian distribution for the passing ions.

Fig. 6 Electron and ion density for the region between the plug and the barrier minimum versus ϕ and B. The Region IV electrons have temperature T_{ec}.

Fig. 7 Same as Fig. 6 except that the Region IV electrons have temperature T_{ep} and a Maxwellian distribution for the passing ions. The three intersections indicate a multiple-valued solution for the potential.

Fig. 8 Calculated electrostatic potential profile in the thermal barrier for the magnetic field profile shown. This calculation assumes $T_{ec}=T_{ic}=T_c$ and no trapped ions in the barrier.

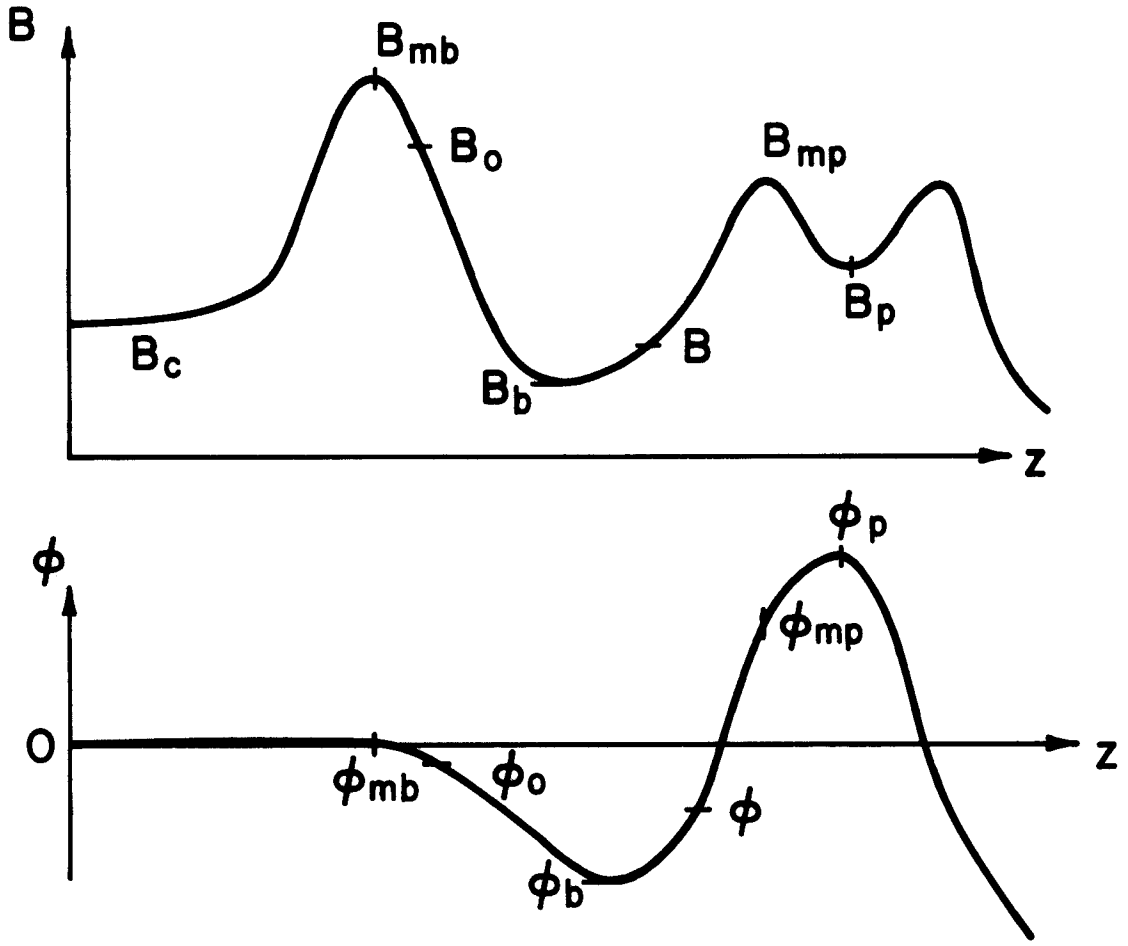

FIG. 1

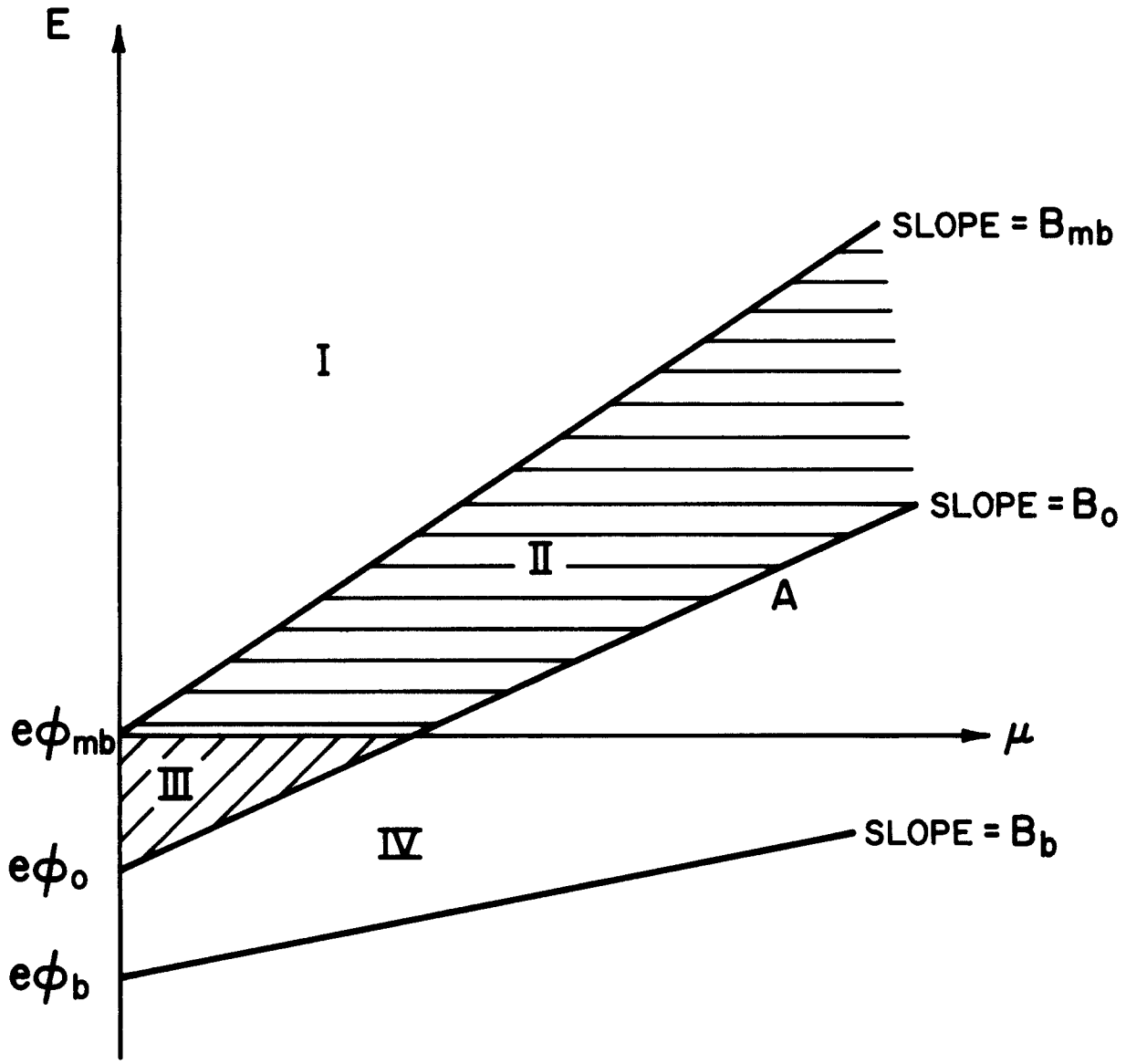
E
SLOPE = B_{mb}
I
SLOPE = B_o
II
A
$e\phi_{mb}$
μ
III
IV
SLOPE = B_b
$e\phi_o$
$e\phi_b$

FIG. 2

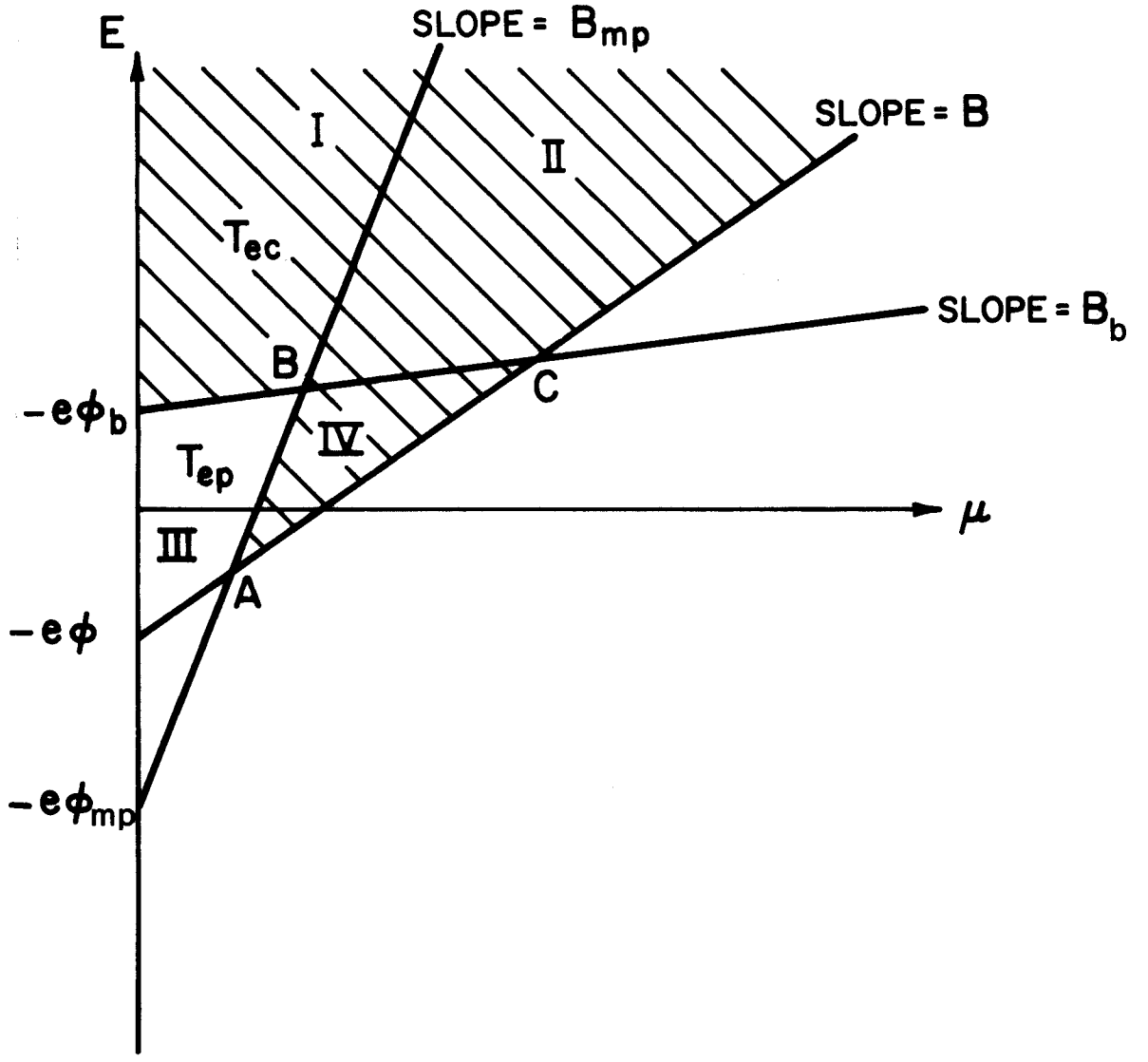
E
SLOPE = B_{mp}
SLOPE = B
SLOPE = B_b
I
II
III
IV
T_{ec}
T_{ep}
B
C
A
$-e\phi_b$
$-e\phi$
$-e\phi_{mp}$
μ

FIG. 3

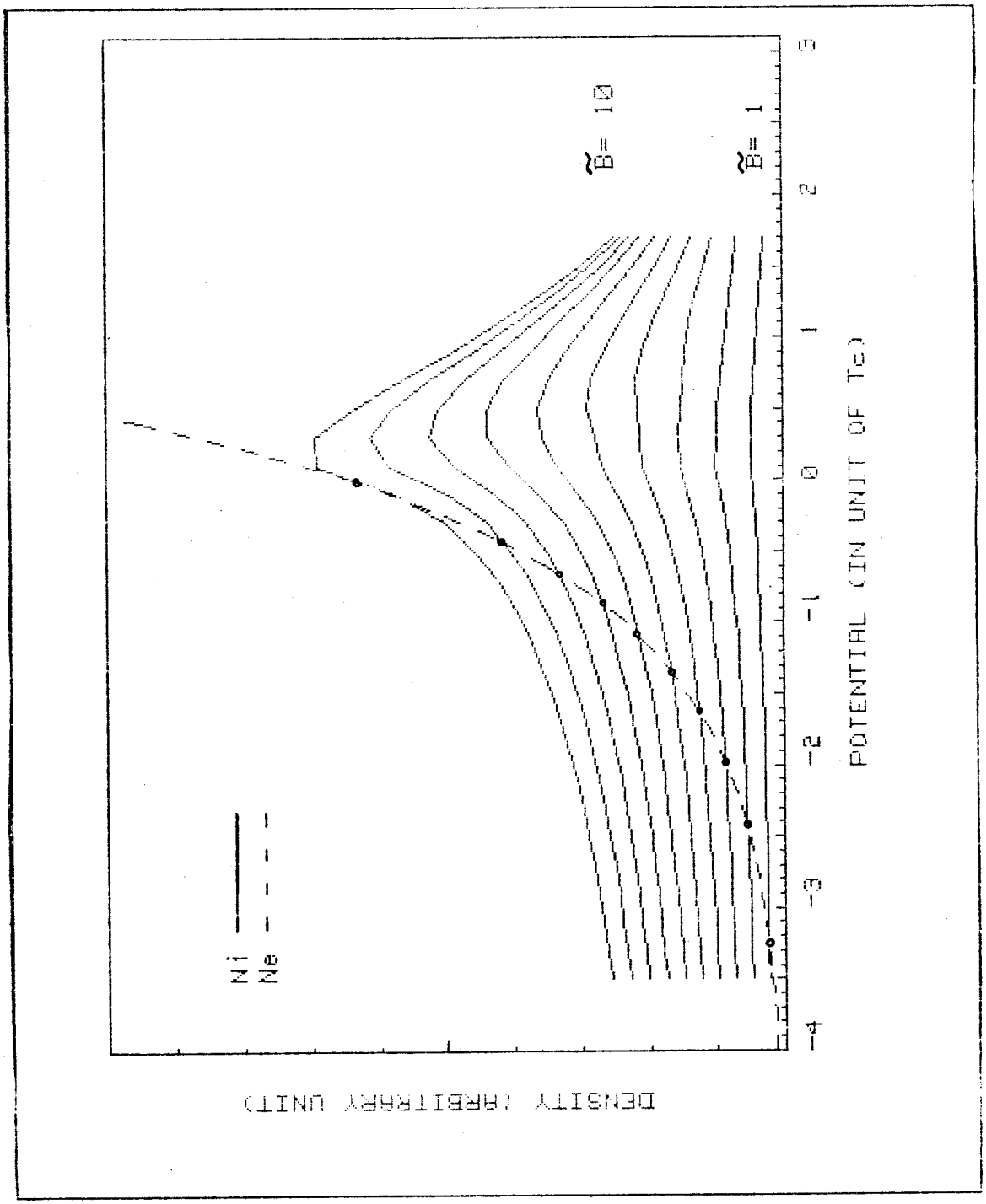
DENSITY (ARBITRARY UNIT)
Ni
Ne
-4
-3
-2
-1
0
1
2
3
POTENTIAL (IN UNIT OF Te)
β= 1
β= 10

Figure 4

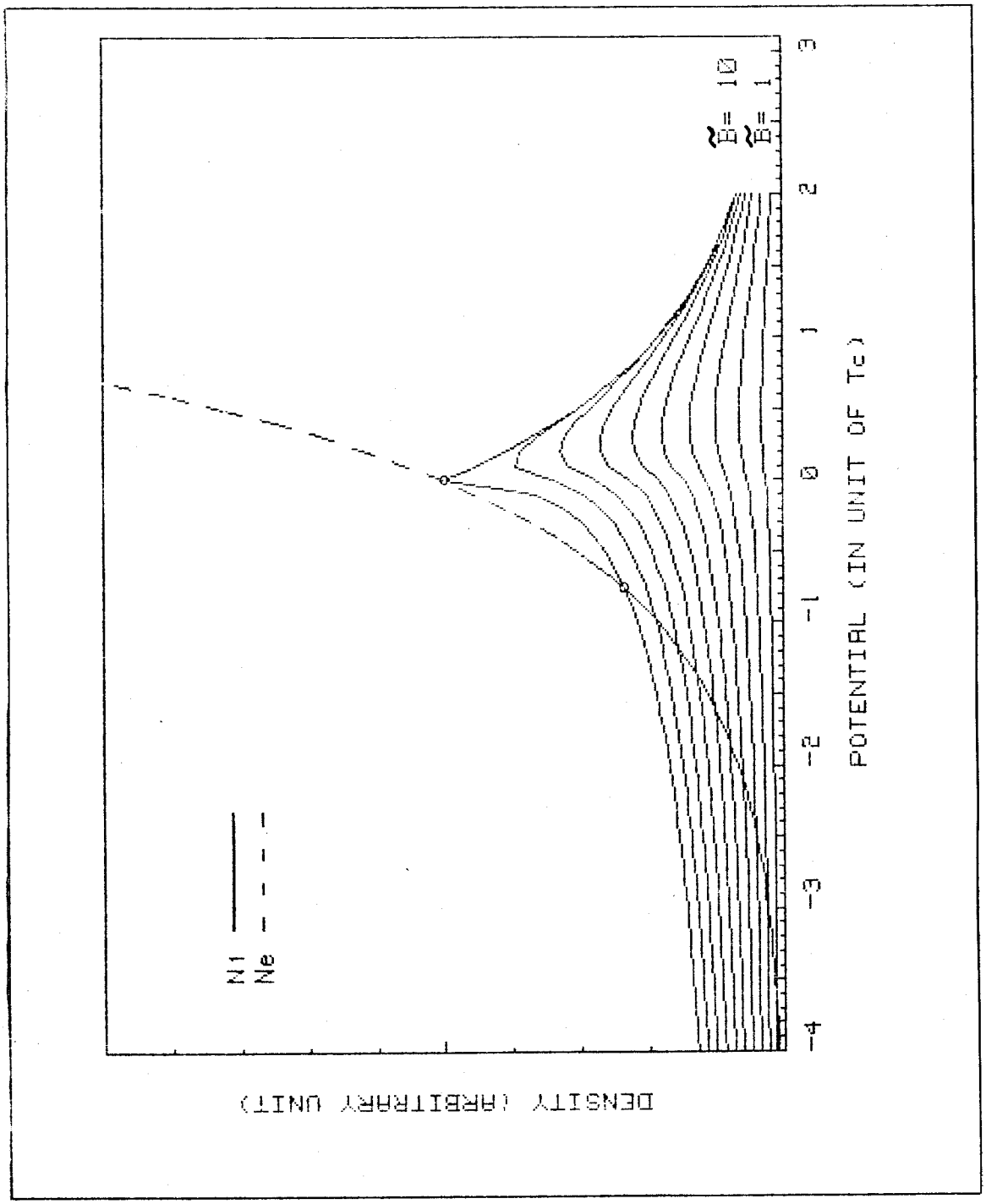
DENSITY (ARBITRARY UNIT)
POTENTIAL (IN UNIT OF Te)
Ni
Ne
β= 10
β= 1
-4
-3
-2
-1
0
1
2
3

Figure 5

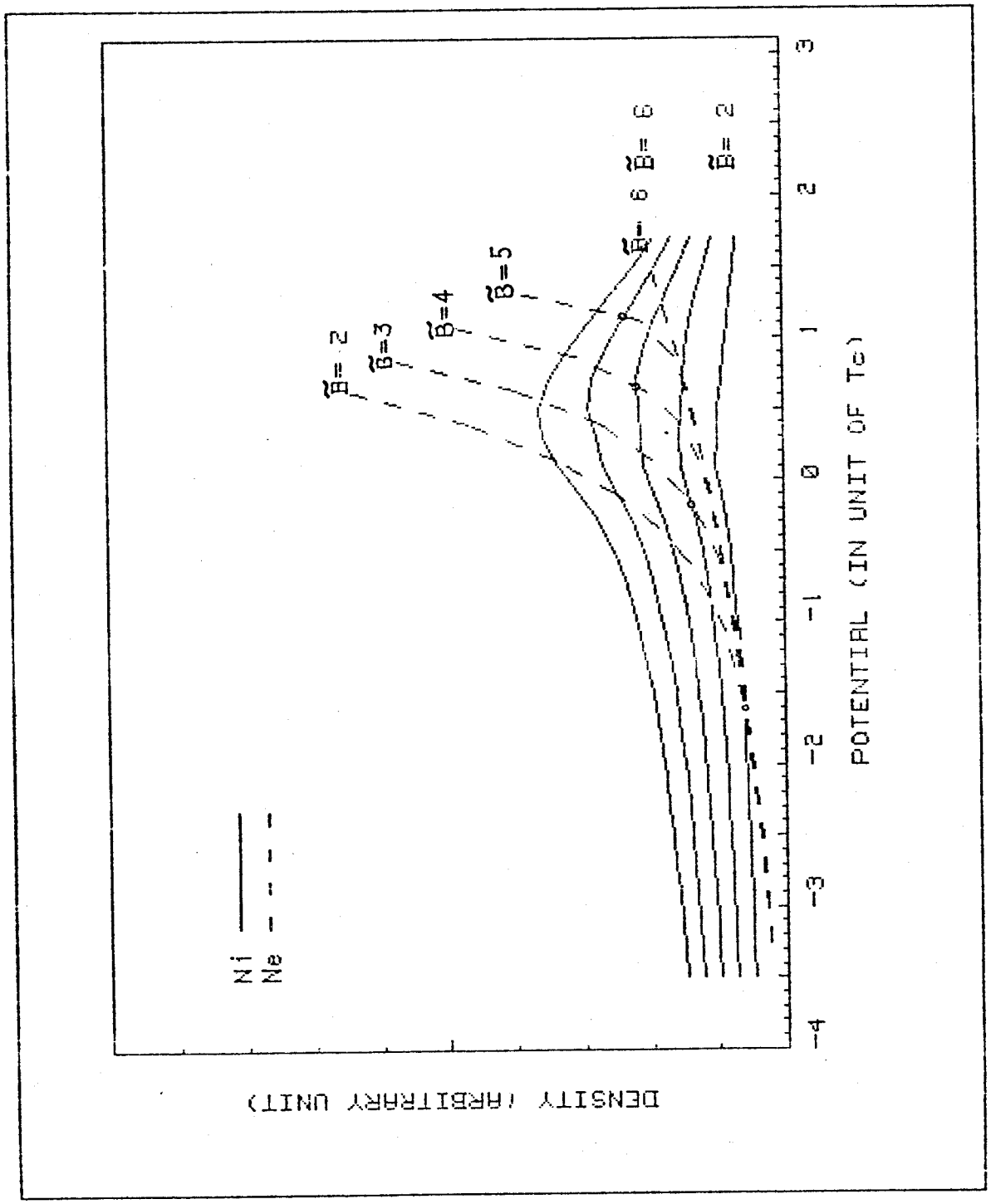
DENSITY (ARBITRARY UNIT)
POTENTIAL (IN UNIT OF Te)
Ni
Ne
B̃= 2
B̃=3
B̃=4
B̃=5
B̃= 6
B̃= 6
B̃= 2
3
2
1
0
-1
-2
-3
-4

Figure 6

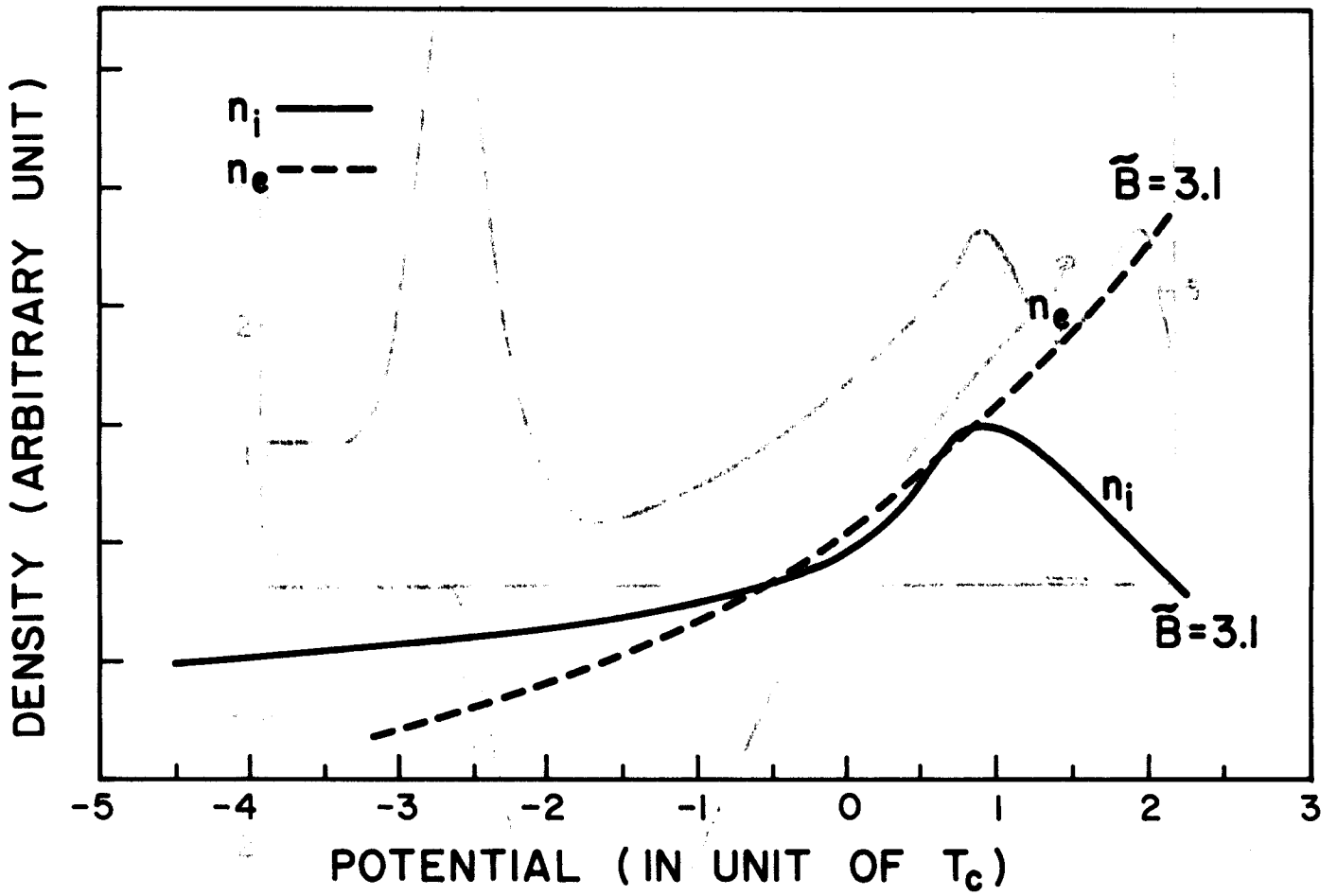
DENSITY (ARBITRARY UNIT)
n_i
n_e
$\tilde{B}=3.1$
n_e
n_i
$\tilde{B}=3.1$
-5
-4
-3
-2
-1
0
1
2
3
POTENTIAL (IN UNIT OF T_c)

FIG. 7

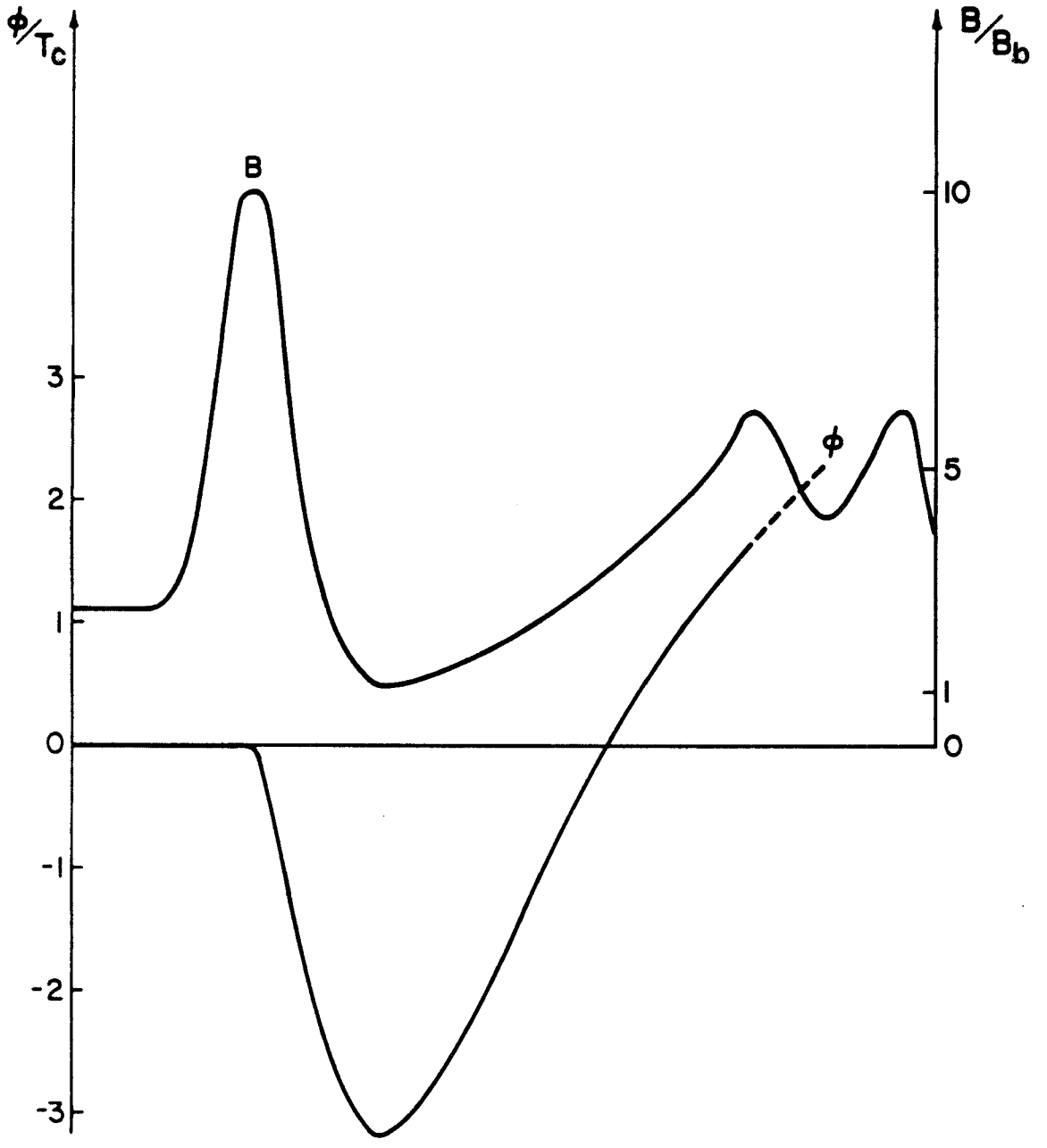

FIG. 8